Optics Communications 283 (2010) 1161–1168

Contents lists available at ScienceDirect

Optics Communications

journal homepage: www.elsevier.com/locate/optcom

Light propagation in nonuniform plasmonic subwavelength waveguide arrays

Massimiliano Guasoni, Matteo Conforti *, Costantino De Angelis

Dipartimento di Elettronica per l'Automazione and Consorzio Interuniversitario per le Scienze Fisiche della Materia, Università di Brescia, via Branze 38, Brescia 25123, Italy

ARTICLE INFO

Article history:
Received 6 August 2009
Received in revised form 21 October 2009
Accepted 29 October 2009

Keywords:
Plasmonics
Waveguide arrays
Discrete diffraction

ABSTRACT

We study light propagation in nanoscale periodic structures composed of dielectric and metal in the visible range. We demonstrate that diffraction curves of nonuniform waveguide arrays can be tailored by varying the geometric and dielectric features of the waveguides. The results obtained from a proper formulation of coupled mode theory for nonuniform arrays are validated through numerical solution of Maxwell equations in frequency domain.

1. Introduction

The miniaturization of photonic devices for confining and guiding electromagnetic energy down to nanometer scale is one of the biggest challenges for the information technology industries [1]. In the last years, photonic crystals technology allowed to gain one order of magnitude in the miniaturization of components such as waveguides and couplers with respect to conventional (i.e. based on total internal reflection) optics. However when the size of a conventional optical circuit is reduced to the nanoscale, the propagation of light is limited by diffraction. One way to overcome this limit is through surface plasmon polaritons [2], which are evanescent waves trapped at the interface between a medium with positive real part of dielectric constant and one with negative real part of dielectric constant, such as metals in the visible range. Even though this phenomenon has been known for a long time, in the last years there is a renewed interest in this field, mainly motivated by the wide range of potential applications that sweep from the realization of biologic nanosensors [3], to sub-wavelength imaging [4], to the merging of electronic circuits to photonic devices [5].

On the other hand, control of light propagation by means of periodic photonic structures is a fundamental issue that is attracting a lot of interest in the scientific community. In particular, arrays of evanescently coupled waveguides are unique structures that exhibit the peculiar properties of discrete systems. Indeed, light propagation in waveguide arrays is characterized by strong confinement of the field into the individual waveguides and the observable exotic phenomena are due to the weak coupling between the waveguides. As a result, modes of the whole structure can be approximated by a superposition of a discrete set of localized modes, thus light propagation can be considered truly discretized [6,7]. Recently there is a great research effort in the field of discrete effects in plasmonic structures, and some peculiar outcome of discreteness were reported for metal–dielectric waveguide arrays, for example Bloch oscillations [8–10], negative refraction [11] diffraction management [12] and subwavelength focusing [13,14].

Nonuniform waveguide arrays have received increasing attention, since a more complex engineering of the periodic structure can provide further degrees of freedom. In this context, the first reported example concerns the usage of zigzag waveguide arrays (i.e., the cascade of arrays characterized by alternating tilt angles) in order to obtain diffraction management. Binary arrays composed of waveguides with alternating widths have been thoroughly studied [15,16] since they exhibit interesting features, such as double refraction, due to their intrinsic two-band nature.

In the present work we study the behavior of nonuniform metal–dielectric waveguide arrays composed of waveguides with different dielectric cores, that determine strong variations of the coupling coefficients. Coupled mode theory (CMT) is extended in order to deal with plasmonic modes and varying coupling coefficients, and further improvements are proposed in order to take into account the different widths of the two array bands. Moreover, we demonstrate that the ability to control the magnitude of the coupling between the waveguides opens the way to the design of binary waveguide arrays with unusual properties, such as almost flat diffraction curves, that are required, for example, to achieve self collimation [17]. Finite element solution of Maxwell equations in nonuniform plasmonic waveguide arrays are reported in order to assess the validity of the analytical treatment.

* Corresponding author.
E-mail address: matteo.conforti@ing.unibs.it (M. Conforti).

0030-4018/$ - see front matter © 2009 Elsevier B.V. All rights reserved.
doi:10.1016/j.optcom.2009.10.103

The paper is organized as follows. After this Introduction, in Section 2 we introduce the nonuniform arrays and report some results of the standard CMT. In Section 3 we develop an extension of coupled mode theory for nonuniform waveguide arrays that exploits the unsymmetric coupler as the fundamental cell; this extension is motivated by the unacceptable low accuracy of the standard CMT for nonuniform plasmonic waveguide arrays. In Section 4, we analyze the peculiar field shape in binary plasmonic arrays and its consequences related to the calculation of coupling coefficients. In Section 5 we exploit the theoretical results of previous sections to engineer diffraction in nonuniform waveguide arrays, reporting as a relevant example the design of arrays characterized by a flat diffraction curve. We end with the conclusion in Section 6.

2. Nonuniform plasmonic arrays

We consider a one dimensional (1D) array formed by the alternation of two dielectric layers (cores) divided by a metallic one (cladding), as sketched in Fig. 1. In a CMT approach we can consider, as basic cell, the single isolated waveguide formed by a dielectric layer surrounded by metal (Fig. 2). Let us call $\varepsilon_1, \varepsilon_2$ and ε_m the relative dielectric constants of dielectrics and metal in the array, and $2a$ and $2b$ the widths of metallic and dielectric layers, respectively. Metal dielectric constant ε_m is calculated by means of Drude model, i.e. $\varepsilon_m = 1 - \omega_p^2/(\omega^2 - i\gamma\omega)$, where ω_p and γ are the plasma and collision frequency of the metal, respectively. Supposing that $\varepsilon_2 > \varepsilon_1$ (from here and for the rest of the article), we work at frequencies such that $\omega < \omega_p/\sqrt{1+\varepsilon_2}$. Under this condition, the fundamental mode of the single waveguides is TM-even and can be expressed as a sum of decaying exponentials both in dielectric and metal; if $2b$ is sufficiently small the guides are monomodal, that is the necessary condition to obtain a bimodal array. Indeed the array supports two different modes since the alternated guides have different propagation constants β_1 and β_2. According to CMT model, diffraction functions of the two array modes are [15]:

$$k_{z(1,2)}(k) = \frac{\beta_1 + \beta_2}{2} \pm \sqrt{\left(\frac{\beta_1 - \beta_2}{2}\right)^2 + 4C^2 \cos\left(\frac{k}{2}\right)}, \tag{1}$$

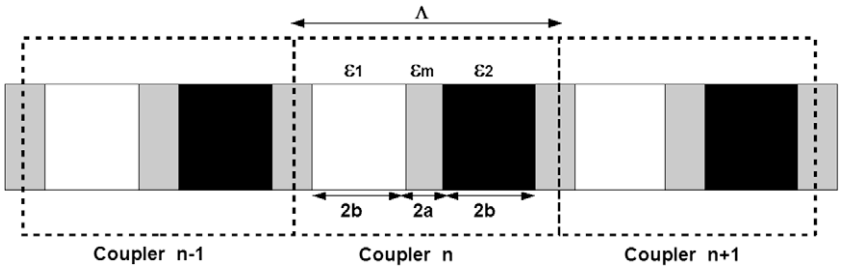

Fig. 1. The plasmonic array studied in this paper. Two cores with dielectric constant ε_1 and ε_2 (white and black respectively) are alternated and divided by a metal layer (grey) whose dielectric constant is ε_m. Width of cores is $2b$, width of metal layers is $2a$. The fundamental period Λ is $4a + 4b$. Dashed rectangles surround three consecutive basic cells of the array, that according to the CMT developed in this paper are plasmonic couplers.

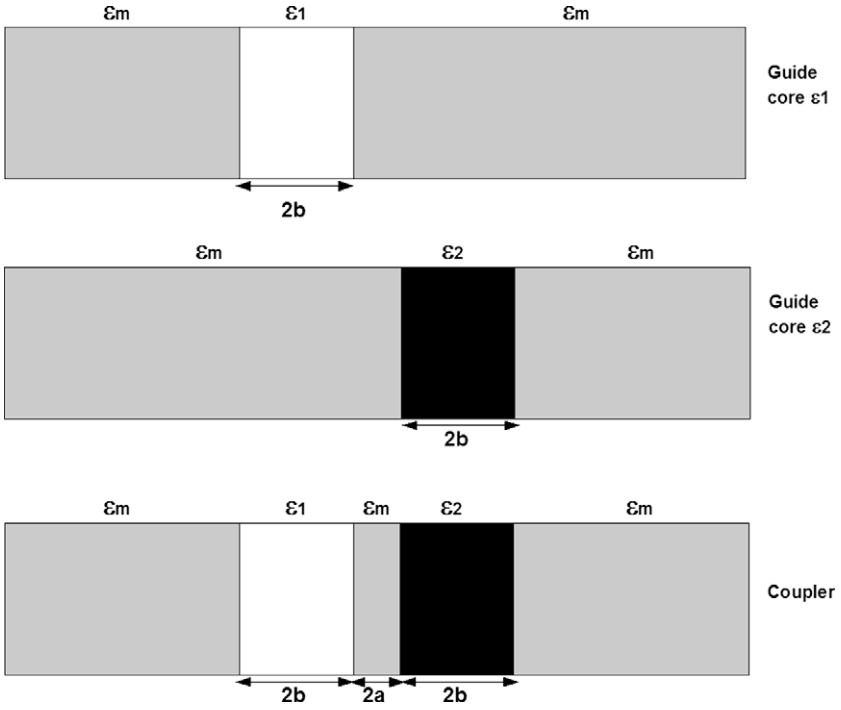

Fig. 2. In the upper and in the center figure two single plasmonic guides are shown. The cores (width $2b$) have dielectric constant ε_1 and ε_2 respectively, and are surrounded by metal with dielectric constant ε_m. In the lower figure there is the coupler used as basic cell in the CMT developed in this paper. Two cores (width $2b$) with dielectric constant ε_1 and ε_2, and divided by a metal layer (width $2a$, dielectric constant ε_m), are surrounded by metal.

where k is the tilt angle normalized with respect to the period of the array ($-\pi < k < \pi$) and C is the coupling coefficient between modes of adjacent waveguides, whose value is [18]:

$$C = \omega\varepsilon_0 \int_{-\infty}^{+\infty} \left[\varepsilon_{arr}(x) - \varepsilon_{g1}(x)\right] E_{x1}(x) E_{x2}^*(x)\, dx + \omega\varepsilon_0 \int_{-\infty}^{+\infty} \frac{\varepsilon_{g2}(x)\left[\varepsilon_{arr}(x) - \varepsilon_{g1}(x)\right]}{\varepsilon_{arr}(x)} E_{z1}(x) E_{z2}^*(x)\, dx. \quad (2)$$

In Eq. (2) ε_0 is the dielectric constant of vacuum, E_{x1}, E_{x2}, E_{z1} and E_{z2} are the modal electric fields of the two isolated waveguides, $\varepsilon_{g1}(x)$ and $\varepsilon_{g2}(x)$ are the dielectric profiles of the two unperturbed waveguides and $\varepsilon_{arr}(x)$ is the dielectric profile of the whole array.

Looking at Eq. (1) we see that by controlling $\Delta\beta = (\beta_1 - \beta_2)/2$ and C we can obtain diffraction curves with very different amplitudes, where for amplitude we mean $k_{z(1,2)}(\pi) - k_{z(1,2)}(0)$. For example when $\Delta\beta \gg C$, diffraction curves become nearly flat. The propagation constant β of a single guide with relative dielectric constant ε and width $2b$ at pulsations ω that satisfy the inequality $\varepsilon/|\varepsilon_m(\omega)| < 0.5$ is well approximated by Eq. (3) (see Appendix):

$$\beta \approx \sqrt{\varepsilon}\sqrt{\left(\frac{w}{c_0}\right)^2 + \left(\frac{w_p}{|\varepsilon_m| c_0 b}\right)}, \quad (3)$$

where c_0 is light speed in vacuum. It's easy to note that β is very sensitive to ε, so that a sensible difference $\Delta\beta$ arises ($\beta_2/\beta_1 = \sqrt{\varepsilon_2/\varepsilon_1}$) by coupling waveguides with cores with different dielectric constant ε_1 and ε_2. In contrast, the dependence of β on the width b is usually weaker than the dependence on ε. For example, if we use silver (neglecting losses: $w_p = 13.6884e15$ rad/s,$\gamma = 0$ rad/s), at any pulsation smaller than $\omega_p/\sqrt{1+\varepsilon}$, β is almost independent on b, for $b > 40$ nm : so $\Delta\beta$ will be quite small when coupling waveguides with the same dielectric but different width.

3. Coupled mode theory for plasmonic arrays

It's well known that CMT gives good results when the modes of two coupled waveguides are, with good approximation, a linear combination of the modes of the single unperturbed waveguides. From Eq. (1) we derive that the second array mode has a diffraction curve $k_{z2}(k)$ whose values can be smaller than $\omega\sqrt{\varepsilon_2}/c_0$, implying that field becomes sinusoidal in the cores of the waveguides with dielectric ε_2 (for large enough values of C).

In these conditions a linear combination of single waveguides modes (that are combination of exponentials in the cores) cannot well approximate the real array mode, making the value of $k_{z2}(k)$ calculated from Eq. (1) unreliable. To overcome this problem we consider a refined CMT model where the single cell of the array consists of two adjacent waveguides (i.e. a waveguide coupler) with dielectrics ε_1 and ε_2, respectively (Fig. 2). We expect this alternative formulation of CMT to work better, because it takes into account the effective fundamental basic cell of the nonuniform array (that is the coupler). We will consider linear combination of the coupler modes, that can be sinusoidal in waveguides with dielectric ε_2, approximating better the second array mode. Let us consider bimodal couplers (any coupler has at least two TM-modes), and let us use a CMT model in which array modes are linear combinations of the two modes of all the couplers in the array, so that the total transverse electric field $E_x(x,z)$ can be written as:

$$E_x(x,z) = \sum_n A_{n,a}(z) E_{x(n,a)}(x) + A_{n,b}(z) E_{x(n,b)}(x) + E_{res}(x), \quad (4)$$

where $E_{x(n,a)}(x)$ and $E_{x(n,b)}(x)$ are the two modes (denoted with a and b) of the nth coupler in the array, $A_{n,a}(z)$ and $A_{n,b}(z)$ are their related coefficients in the linear combination and $E_{res}(x)$ is the residual field. Supposing that the residual field is negligible and following the treatment reported in [18], we obtain the relations below:

$$A'_{n,a} + R_{a1,a2}A'_{n+1,a} + R_{a1,a0}A'_{n-1,a} + R_{a1,b2}A'_{n+1,b} + R_{a1,b0}A'_{n-1,b} = i(\beta_a + k_{a1,a1})A_{n,a} + iC_{a1,b1}A_{n,b} + iC_{a1,a2}A_{n+1,a} + iC_{a1,a0}A_{n-1,a} + iC_{a1,b2}A_{n+1,b} + iC_{a1,b0}A_{n-1,b}, \quad (5)$$

$$A'_{n,b} + R_{b1,b2}A'_{n+1,b} + R_{b1,b0}A'_{n-1,b} + R_{b1,a2}A'_{n+1,a} + R_{b1,a0}A'_{n-1,a} = i(\beta_b + k_{b1,b1})A_{n,b} + iC_{b1,a1}A_{n,a} + iC_{b1,b2}A_{n+1,b} + iC_{b1,b0}A_{n-1,b} + iC_{b1,a2}A_{n+1,a} + iC_{b1,a0}A_{n-1,a}. \quad (6)$$

In Eqs. (5) and (6) $A'_{n,i}(i = a, b)$ is the derivative respect to z of $A_{n,i}$. Any term $R_{i1,jl}$ is the correlation between mode i in the coupler n and mode j in coupler $m = n + l - 1$ ($l = 0$ with reference to the coupler at the left of the coupler n and $l = 1$ with reference to the coupler n and $l = 2$ with reference to the coupler at its right, see Fig. 1), that is:

$$R_{i1,jl} = \int_{-\infty}^{+\infty} E_{x(n,i)}(x) H_{y(m,j)}^*(x)\, dx. \quad (7)$$

Under the normalization condition $R_{i1,i1} = 1$, while $R_{i1,j1} = 0 (i \neq j)$ because different modes in the same coupler are orthogonal. β_a and β_b are the propagation constants of modes a and b in any basic unperturbed coupler, while any term $C_{i1,jl}$ is the coupling coefficient between mode i in the coupler n and mode j in coupler $m = n + l - 1$. This coefficient can be written as:

$$C_{i1,jl} = \beta_i R_{i1,jl} + k_{i1,jl},, \quad (8)$$

where the term $k_{i1,jl}$ is:

$$k_{i1,jl} = \omega\varepsilon_0 \int_{-\infty}^{+\infty} \left\{ [\varepsilon_{arr}(x) - \varepsilon_{cn}(x)] E_{x(n,i)}(x) E_{x(m,j)}^*(x) + \frac{\varepsilon_{cm}(x)[\varepsilon_{arr}(x) - \varepsilon_{cn}(x)]}{\varepsilon_{arr}(x)} E_{z(n,i)}(x) E_{z(m,j)}^*(x) \right\} dx, \quad (9)$$

where $\varepsilon_{cn}(x)$ and $\varepsilon_{cm}(x)$ are the transverse dielectric profiles of adjacent and unperturbed couplers n and m, while $\varepsilon_{arr}(x)$ is the transverse profile of the whole array.

Using as solutions $A_{n,a} = Ae^{ikn + ik_z z}$ and $A_{n,b} = Be^{ikn + ik_z z}$ ($-\pi < k < \pi$) we can rewrite Eq. (5) and Eq. (6) in matrix form:

$$\overline{R}\begin{bmatrix} A \\ B \end{bmatrix} k_z = \overline{C}\begin{bmatrix} A \\ B \end{bmatrix}, \quad (10)$$

where:

$$\overline{R} = \begin{bmatrix} P_{11} & P_{12} \\ P_{21} & P_{22} \end{bmatrix}, \quad \overline{C} = \begin{bmatrix} Q_{11} & Q_{12} \\ Q_{21} & Q_{22} \end{bmatrix} \quad (11)$$

with

$$\begin{aligned} Q_{11} &= \beta_a + k_{a1,a1} + C_{a1,a2}e^{ik} + C_{a1,a0}e^{-ik}, \\ Q_{12} &= C_{a1,b1} + C_{a1,b2}e^{ik} + C_{a1,b0}e^{-ik}, \\ Q_{21} &= C_{b1,a1} + C_{b1,a2}e^{ik} + C_{b1,a0}e^{-ik}, \\ Q_{22} &= \beta_b + k_{b1,b1} + C_{b1,b2}e^{ik} + C_{b1,b0}e^{-ik}, \\ P_{11} &= 1 + R_{a1,a2}e^{ik} + R_{a1,a0}e^{-ik}, \\ P_{12} &= R_{a1,b2}e^{ik} + R_{a1,b0}e^{-ik}, \\ P_{21} &= R_{b1,a2}e^{ik} + R_{b1,a0}e^{-ik}, \\ P_{22} &= 1 + R_{b1,b2}e^{ik} + R_{b1,b0}e^{-ik}. \end{aligned}$$

Diffraction curves $k_z(k)$ are the eigenvalues of $\overline{R}^{-1}\overline{C}$; being coefficients $R_{ix,jy} \ll 1$ in Eq. (11), we can well approximate $\overline{R}^{-1} \approx (2I - \overline{R})$. In the product $(2I - \overline{R})\overline{C}$ we can neglect all terms different

from $C_{i1,jl}, \beta_a, \beta_b, \beta_a R_{i1,jl}$ and $\beta_b R_{i1,jl}$ because they are much smaller. In this way, matrix $(2I-\overline{R})\overline{C}$ becomes:

$$(2I-\overline{R})\overline{C} = \begin{bmatrix} M_{11} & M_{12} \\ M_{21} & M_{22} \end{bmatrix}, \tag{12}$$

where

$$M_{11} = \beta_a + k_{a1,a1} + k_{a1,a2}e^{ik} + k_{a1,a0}e^{-ik},$$
$$M_{12} = k_{a1,b1} + (k_{a1,b2} + 2\Delta\beta R_{a1,b2})e^{ik} + (k_{a1,b0} + 2\Delta\beta R_{a1,b0})e^{-ik}$$
$$M_{21} = k_{b1,a1} + (k_{b1,a2} - 2\Delta\beta R_{b1,a2})e^{ik} + (k_{b1,a0} - 2\Delta\beta R_{b1,a0})e^{-ik}$$
$$M_{22} = \beta_b + k_{b1,b1} + k_{b1,b2}e^{ik} + k_{b1,b0}e^{-ik}$$

and $\Delta\beta = (\beta_a - \beta_b)/2$.

If we neglect the residual field $E_{res}(x)$, the system conserves the energy, implying that $\overline{R}^{-1}\overline{C}$ must be hermitian. This property imposes the following equalities:

$$k_{a1,a2} = k_{a1,a0} = C_a,$$
$$k_{b1,b2} = k_{b1,b0} = C_b,$$
$$k_{a1,b2} + 2\Delta\beta R_{a1,b2} = k_{b1,a0} - 2\Delta\beta R_{b1,a0} = C_{ab},$$
$$k_{a1,b0} + 2\Delta\beta R_{a1,b0} = k_{b1,a2} - 2\Delta\beta R_{b1,a2} = C_{ba},$$
$$k_{a1,b1} = k_{b1,a1} = C.$$

Moreover, calling $\beta_a + k_{a1,a1} = \bar{\beta}_a$ and $\beta_b + k_{b1,b1} = \bar{\beta}_b$, we can rewrite (12) in this way:

$$(2I-\overline{R})\overline{C} = \begin{bmatrix} \bar{\beta}_a + 2C_a\cos(k) & C + C_{ab}e^{ik} + C_{ba}e^{-ik} \\ C + C_{ba}e^{ik} + C_{ab}e^{-ik} & \bar{\beta}_b + 2C_b\cos(k) \end{bmatrix}. \tag{13}$$

Diffraction curves are the eigenvalues of (13):

$$k_{z(1,2)} = \frac{\bar{\beta}_a + \bar{\beta}_b}{2} + (C_a + C_b)\cos(k) \pm \sqrt{\left[\frac{\bar{\beta}_a - \bar{\beta}_b}{2} + (C_a - C_b)\cos(k)\right]^2 + |C + C_{ab}e^{ik} + C_{ba}e^{-ik}|^2}. \tag{14}$$

Even when difference $(\varepsilon_2 - \varepsilon_1)$ is small, the two modes of any coupler concentrate energy in a different way: the first confine the most part of energy in the core with dielectric constant ε_2, while the second in the core with dielectric ε_1, so that the term $(\bar{\beta}_a - \bar{\beta}_b)$ increases and coefficients C, C_{ab} and C_{ba} becomes negligible respect to $[(\bar{\beta}_a - \bar{\beta}_b)/2 + (C_a - C_b)\cos(k)]^2$, implying:

$$k_{z1} = \bar{\beta}_a + 2C_a\cos(k),$$
$$k_{z2} = \bar{\beta}_b + 2C_b\cos(k). \tag{15}$$

That is a very simple solution where the two diffraction curves depend only on the coupling between same modes in two adjacent couplers. Their amplitudes are respectively $4C_a$ and $4C_b$, and they can take very different values, in contrast to what results from Eq. (1). We must emphasize that the procedure reported in this paper can be applied to the study of any type of binary array (i.e. it works equally well for both dielectric and plasmonic arrays); on the contrary, as already explained above, the standard procedure used in the analysis of binary dielectric waveguide arrays [19] would not work for our plasmonic binary array.

4. Modes and energy concentration in plasmonic arrays

Now we want to show that the coupling coefficients depend quite exclusively on how field of the unperturbed basic coupler concentrates at the metal–dielectric interfaces. This fact allow us to deeply understand the link between nonuniformity of the array $(\varepsilon_2 \neq \varepsilon_1)$ and its diffraction curves. Let us call g_1, g_2 and g_m the regions with dielectric $\varepsilon_1, \varepsilon_2$ and ε_m in the coupler (Fig. 2), and let us start with observing that the first coupler mode is very similar to the mode of the single isolated guide with core ε_2, excluding the region g_1. We can then approximate the first coupler mode in all regions except g_1 with the mode of the single guide with core ε_2. An analogous argument holds true for the second coupler mode. Coupling coefficient $C_a = k_{a1,a0}$ can be very well approximated considering only the fields overlapping in region g_2 of coupler $(n-1)$ (see Fig. 3):

$$C_a \approx \underbrace{\omega\varepsilon_0(\varepsilon_2 - \varepsilon_m)\int_{g2,n-1} E_{x(n,a)}(x)E_{x(n-1,a)}(x)^*}_{C'_a} + \underbrace{\omega\varepsilon_0(\varepsilon_2 - \varepsilon_m)\int_{g2,n-1} E_{z(n,a)}(x)E_{z(n-1,a)}(x)^*}_{C''_a}, \tag{16}$$

where we distinguish the overlapping between the x and z components of electric fields (C'_a and C''_a, respectively). Subscript $(g_2, n-1)$ refers to the region g_2 of coupler $(n-1)$. Let us consider now an array with dielectrics ε_1 and ε_2, and let us study nonuniformity effects by varying ε_2 keeping ε_1 fixed. In $(g_2, n-1)$ the fields $E_{x(n,a)}(x, \varepsilon_2)$ and $E_{z(n,a)}(x, \varepsilon_2)$ behave nearly such as the mode of the single guide with core ε_2, that decays in metal with constant T_m (see Appendix). Being T_m practically independent on ε_2, also the field $E_{x(n,a)}(x, \varepsilon_2)$ is quite independent on ε_2 in $(g_2, n-1)$ except for a constant, so that we can write $E_{x(n,a)}(x, \varepsilon_2) \approx E_{x(n,a)}(x, \varepsilon_1)M^e_{x(L,a)}(\varepsilon_2)$, where $M^e_{x(L,a)}(\varepsilon_2)$ is the magnitude of the transverse electric field of the coupler mode a at the external left interface and, by definition, $M^e_{x(L,a)}(\varepsilon_1) = 1$ (see Fig. 4). For the same fact, $E_{z(n,a)}(x, \varepsilon_2) \approx E_{z(n,a)}(x, \varepsilon_1)M^e_{z(L,a)}(\varepsilon_2)$, where $M^e_{z(L,a)}(\varepsilon_2)$ is the value of the longitudinal electric field of coupler mode a at the external left interface.

Similar arguments hold true for fields $E_{x(n-1,a)}(x, \varepsilon_2)$ and $E_{z(n-1,a)}(x, \varepsilon_2)$: in $(g_2, n-1)$ they are sum of evanescent waves decaying with constant T_d (see Appendix) that does not vary too much as function of ε_2 (when the array is bimodal); so using $E_{x(n-1,a)}(x, \varepsilon_2) \approx E_{x(n-1,a)}(x, \varepsilon_1)M^i_{x(R,a)}(\varepsilon_2)$ and $E_{z(n-1,a)}(x, \varepsilon_2) \approx E_{z(n-1,a)}(x, \varepsilon_1)M^i_{z(R,a)}(\varepsilon_2)$ we approximate very well Eq. (16), being $M^i_{x(R,a)}(\varepsilon_2)$ and $M^i_{z(R,a)}(\varepsilon_2)$ the values of the transverse and longitudinal electric field of the coupler mode a at the internal right

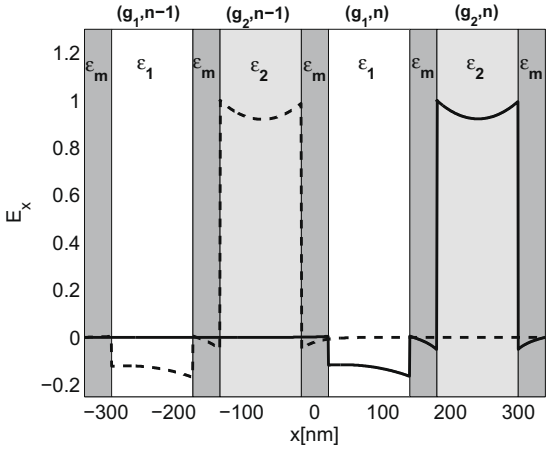

Fig. 3. The array is shown together with transverse electric field E_x of modes a of couplers $n-1$ and n (dotted and solid lines, respectively), that are $E_{x(n-1,a)}$ and $E_{x(n,a)}$ according to the explanation of Section 4. Regions g_1 and g_2 of each coupler are shown ($(g_1, n-1), (g_2, n-1)$ for coupler $n-1$; $(g_1, n), (g_2, n)$ for coupler n). In the region $(g_1, n-1)$ the modes $E_{x(n-1,a)}$ and $E_{x(n,a)}$ are much smaller than in region $(g_2, n-1)$, so that their overlapping in $(g_1, n-1)$ can be neglected in the calculation of $k_{a1,a0}$ (Eq. (16)). Large discontinuities of the electric field are due to the big dielectric constant change between metal and dielectric.

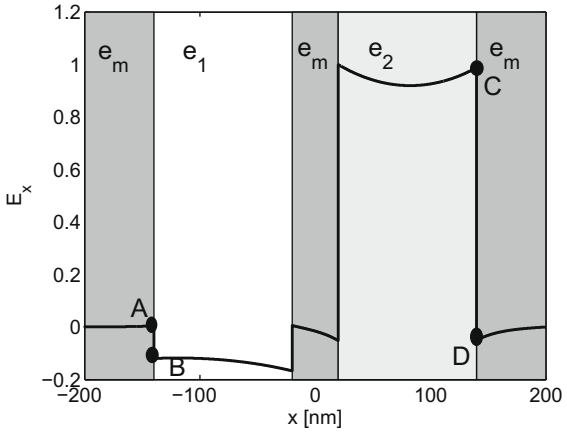

Fig. 4. Solid line is the field E_x of mode a in a coupler with $\varepsilon_1 = 1.0, \varepsilon_2 = 1.5$, width of central metallic layer (ε_m) 40 nm and widths of dielectric layers 120 nm. Wavelength is 750 nm. Black dots denoted with A, B, C, D represent values of field at the interfaces of a coupler used in Eqs. (17) and (18). They are respectively $M^e_{x(L,a)}, M^i_{x(L,a)}, M^i_{x(R,a)}, M^e_{x(R,a)}$.

interface. On the basis of the arguments reported above, we can easily deduct the following relations:

$$\frac{C'_a(\varepsilon_2)}{C'_a(\varepsilon_1)} \approx \frac{\varepsilon_m - \varepsilon_2}{\varepsilon_m - \varepsilon_1} M^e_{x(L,a)}(\varepsilon_2) M^i_{x(R,a)}(\varepsilon_2),$$
$$\frac{C''_a(\varepsilon_2)}{C''_a(\varepsilon_1)} \approx \frac{\varepsilon_m - \varepsilon_2}{\varepsilon_m - \varepsilon_1} M^e_{z(L,a)}(\varepsilon_2) M^i_{z(R,a)}(\varepsilon_2). \quad (17)$$

Reasoning in the same way for $C_b = k_{(b1,b2)}$ we can write:

$$\frac{C'_b(\varepsilon_2)}{C'_b(\varepsilon_1)} \approx M^i_{x(L,b)}(\varepsilon_2) M^e_{x(R,b)}(\varepsilon_2),$$
$$\frac{C''_b(\varepsilon_2)}{C''_b(\varepsilon_1)} \approx M^i_{z(L,b)}(\varepsilon_2) M^e_{z(R,b)}(\varepsilon_2). \quad (18)$$

Eqs. (17) and (18) show how variations of couplings as function of nonuniformity are related only on fields concentration at the interfaces of the unperturbed basic coupler. We note that $C'_a(\varepsilon_2)$ and $C''_a(\varepsilon_2)$ are always decreasing function of ε_2, while $C'_b(\varepsilon_2)$ and $C''_b(\varepsilon_2)$ exhibit a minimum when the condition $k_{z2}(k) \approx \omega\sqrt{\varepsilon_2}/c_0$ is satisfied, corresponding to the threshold between a decaying or oscillating field in the core of the waveguide g_2. This fact is not intuitive, because we could expect that the more the difference $(\varepsilon_2 - \varepsilon_1)$ is increased the more the modes of adjacent couplers are decoupled.

5. Design of a flat-diffraction array in the visible band

In this section we design a nonuniform plasmonic array in order to have flat diffraction curves in all the visible range (450–750 nm) and in order to test all predictions done in the previous sections. Thanks to a flat diffraction curve, is possible to prevent either the beam divergence or diffraction broadening, enabling flexible design of light path in plasmon integrated optics [17].

Dielectric and metal layers of the array are 120 nm and 40 nm wide respectively; $\varepsilon_1 = 1.0$ (air) and metal layers are silver ($\omega_p = 13.61e15$ and $\gamma = 0$, because we can neglect losses for propagation distances that we consider). In Fig. 5 the amplitudes of the two diffraction curves related to the two modes of the array at 450 nm and 750 nm are shown as function of ε_2. We consider only values of ε_2 that allow the array to be bimodal. Difference $(k_{z1}(\pi) - k_{z1}(0))$ is the amplitude of the first diffraction curve (band 1), $(k_{z2}(\pi) - k_{z2}(0))$ is the amplitude of the second (band 2).

Values of $k_{z1}(0), k_{z1}(\pi), k_{z2}(0)$ and $k_{z2}(\pi)$ are calculated by means of Eq. (15), where $\bar{\beta}_a, \bar{\beta}_b, C_a$ and C_b depend on coefficients $\beta_a, \beta_b, k_{a1,a1}, k_{b1,b1}, k_{a1,a2}$ and $k_{b1,b2}$. The first two are the propagation constants of the basic coupler modes and are calculated by means of a mode solver; last four coefficients are calculated using Eq. (9), with E_x and E_z as obtained by the mode solver.

As predicted, the amplitude of the first curve always decreases as function of ε_2, while the second exhibits a minimum of its absolute value. A good choice to obtain a flat second curve in all the visible range is to set $\varepsilon_2 = 1.5$, for which we have nearly the lowest amplitude of band 2 in all the range considered.

In Fig. 6 we show the comparison between the amplitude of diffraction curves in the case of a uniform array ($\varepsilon_1 = 1.0, \varepsilon_2 = 1.0$ or $\varepsilon_1 = 1.5, \varepsilon_2 = 1.5$) and a nonuniform array ($\varepsilon_1 = 1.0, \varepsilon_2 = 1.5$) as function of wavelength: the amplitude is significantly reduced in case of nonuniformity, about 5 times for band 1 and 2–3 times for band 2.

In Fig. 7, in the case of $\varepsilon_1 = 1.0, \varepsilon_2 = 1.5$, we report a comparison between the numerically calculated amplitudes and those predicted by CMT using Eq. (15). Numerical values of $k_{z1}(0), k_{z1}(\pi), k_{z2}(0)$ and $k_{z2}(\pi)$ are calculated with a mode solver.

Relative errors are very small, less then 3% in the worst case. In the case of band 2, numerical and predicted curves are undistinguishable. As expected the amplitudes of both the diffraction curves reduces in modulus by increasing the wavelength. In fact the modulus of the dielectric constant of metal increase with wavelength, enabling a stronger confinement into the waveguides.

In Fig. 8 we report the good agreement between coupling coefficients C_a and C_b calculated with Eq. (9) and those approximated by Eq. (16). In this last case $C'_a(\varepsilon_1), C'_b(\varepsilon_1), C''_a(\varepsilon_1)$ and $C''_b(\varepsilon_1)$ are first calculated with Eq. (16), then $C'_a(\varepsilon_2), C'_b(\varepsilon_2), C''_a(\varepsilon_2)$ and $C''_b(\varepsilon_2)$ are

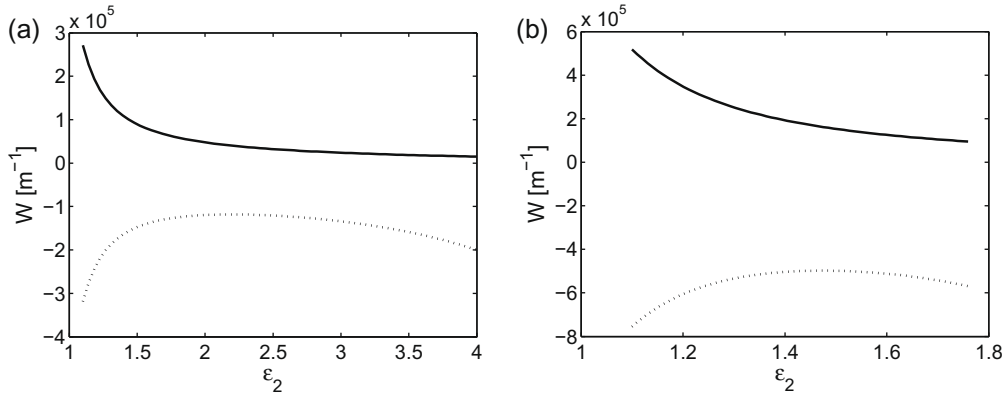

Fig. 5. Amplitude W of the diffraction curves as function of ε_2, when $\varepsilon_1 = 1.0$. Solid lines for band 1, dotted lines for band 2. (a) 750 nm; and (b) 450 nm.

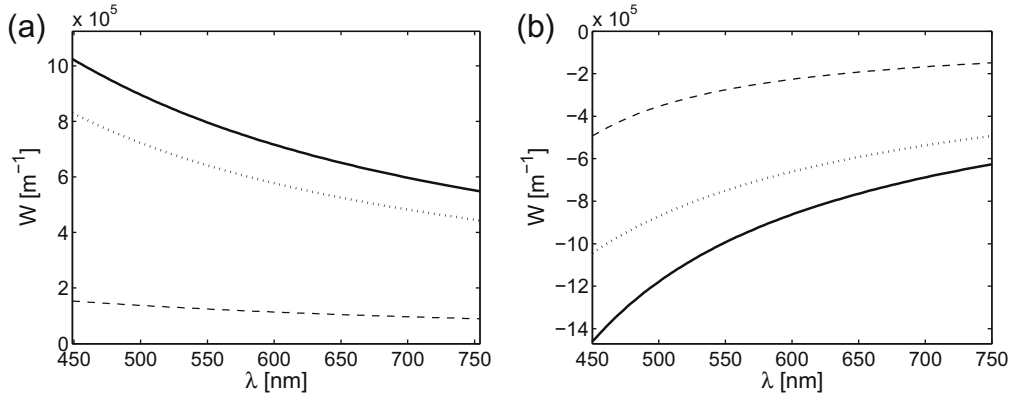

Fig. 6. Amplitude W of the diffraction curves as function of wavelength. Solid line for $\varepsilon_1 = 1.5, \varepsilon_2 = 1.5$; dotted line for $\varepsilon_1 = 1.0, \varepsilon_2 = 1.0$; dashes thin line for $\varepsilon_1 = 1.0, \varepsilon_2 = 1.5$. (a) Band 1; and (b) band 2.

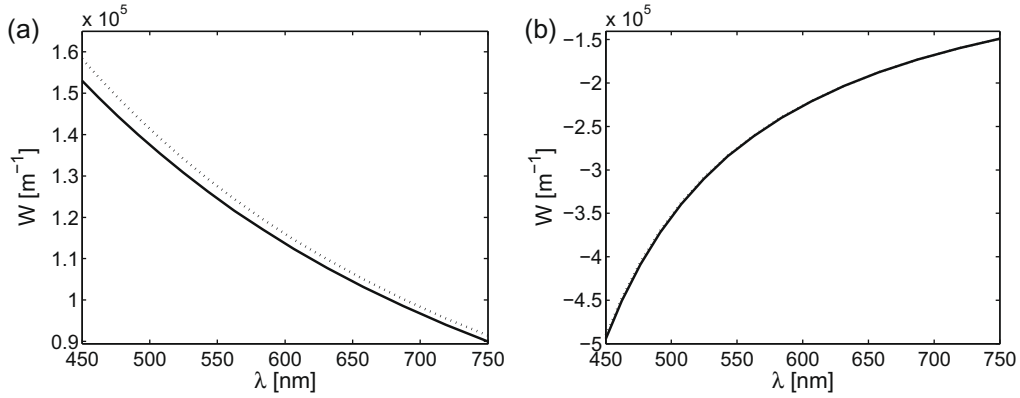

Fig. 7. Amplitudes W of the diffraction curves as function of wavelength when $\varepsilon_1 = 1.0, \varepsilon_2 = 1.5$. Solid line for numerically calculated values; dotted lines for predicted ones (by CMT). (a) Band 1; and (b) band 2.

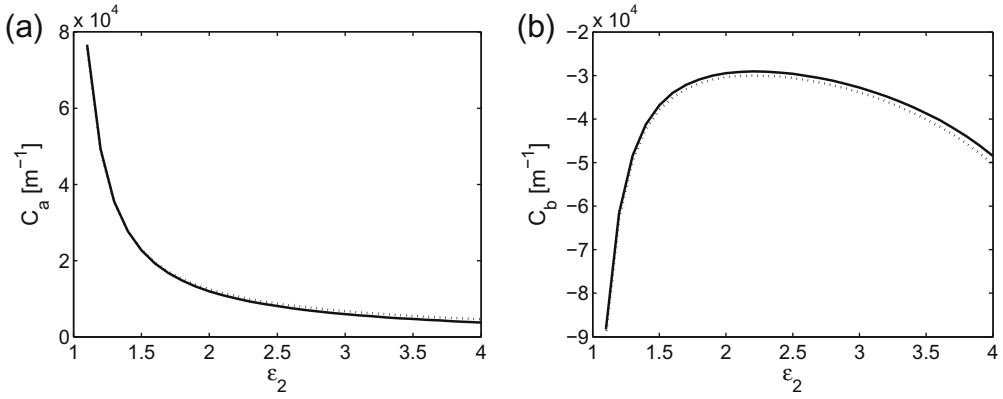

Fig. 8. Coupling coefficients C_a and C_b as function of ε_2, when $\varepsilon_1 = 1.0$. Solid lines represent values calculated with classic CMT model (Eq. (8)); dotted lines represent values $C'_a(\varepsilon_2) + C''_a(\varepsilon_2)$ and $C'_b(\varepsilon_2) + C''_b(\varepsilon_2)$, where $C'_a(\varepsilon_2), C''_a(\varepsilon_2), C'_b(\varepsilon_2)$ and $C''_b(\varepsilon_2)$ are approximated by Eqs. (17) and (18) after calculation of $C'_a(\varepsilon_1), C''_a(\varepsilon_1), C'_b(\varepsilon_1)$ and $C''_b(\varepsilon_1)$. Wavelength is 750 nm. (a) C_a; and (b) C_b.

given by Eqs. (17) and (18), for which fields E_x and E_z need to be calculated by means of a mode solver in order to obtain their magnitudes at the interfaces. C_a is approximated by $(C'_a(\varepsilon_2) + C''_a(\varepsilon_2))$ and C_b by $(C'_b(\varepsilon_2) + C''_b(\varepsilon_2))$.

It is worth noting that the second band coupling constant C_b has a non-monotonic behavior, exhibiting a minimum of the absolute value at around $\varepsilon_2 = 2$, in accordance with Fig. 5.

In Fig. 9 we show numerically calculated diffraction curves at 450 nm and 750 nm, and those predicted by CMT in Eq. (15): also in this case, the agreement is very good. Interestingly enough the curvature changes slightly from 450 nm to 750 nm case, indicating the broadband feature of the diffraction engineering.

In Figs. 10 and 11 we show the solution of Maxwell equation in uniform and nonuniform arrays, obtained by a finite-element

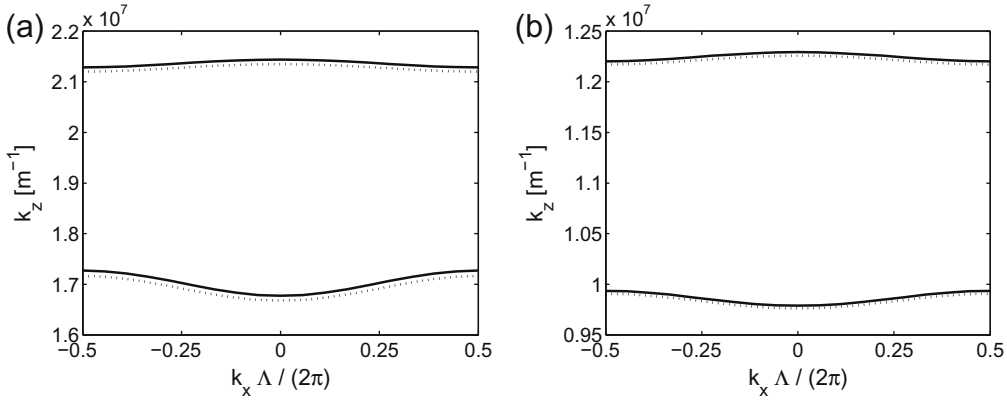

Fig. 9. Diffraction curves $k_z(k_x)$ of the nonuniform array with $2a = 40$ nm, $2b = 120$ nm, $\varepsilon_1 = 1.0, \varepsilon_2 = 1.5$. k_x is normalized with respect to the period Λ of the array. Solid line for numerically calculated values; dotted lines for CMT. (a) 750 nm; and (b) 450 nm.

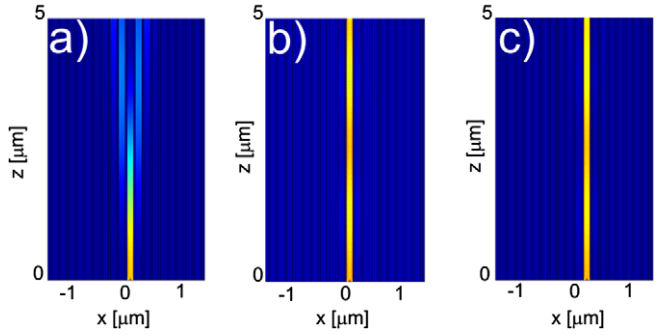

Fig. 10. Propagation in the array with $2a = 40$ nm,$2b = 120$ nm. Single guide excitation. Wavelength λ is 750 nm. (a) $\varepsilon_1 = 1.0, \varepsilon_2 = 1.0$; (b) $\varepsilon_1 = 1.0, \varepsilon_2 = 1.5$, core ε_2 excited; and (c) $\varepsilon_1 = 1.0, \varepsilon_2 = 1.5$, core ε_1 excited.

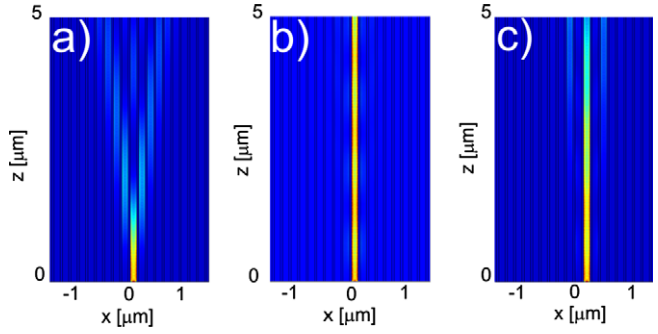

Fig. 11. Same as in Fig. 10, but wavelength λ is 450 nm.

frequency-domain code [20]. In order to test the previous approximations we inject into the arrays a narrow beam, corresponding to a broad spatial spectrum. If the array bands are flat, any plane wave component at the array input should be refracted and diffracted very little, entailing propagation without spatial broadening of the input beam.

In Fig. 10 the input wavelength is set to 750 nm, the propagation length is 5 μm along z direction, and three different cases are compared. On the left propagation in a uniform array with $\varepsilon_1 = \varepsilon_2 = 1.0$ is simulated, and we notice that diffraction effects are much more accentuated than in the central and right figure, where nonuniform case $(\varepsilon_1 = 1.0, \varepsilon_2 = 1.5)$ is considered. In these two last cases, array bands are very flat and for a propagation distance of 5 μm they allow the field to propagate without distortion. In the central figure the core with dielectric ε_1 is excited whereas in the right one the core with dielectric ε_2 is excited. In the first case power is quite totally coupled on band 2, while in second case is quite totally coupled on band 1, so we could notice difference in propagation because the two bands have different amplitudes. Using a wavelength of 750 nm this difference is negligible for a propagation of 5 μm, but becomes noticeable when using a wavelength of 450 nm, as we can see in Fig. 11.

As far as losses are concerned, we verified that the propagation in the diffraction-engineered devices is not influenced at all by including a lossy model for the metal [experimental values [21] gives $\varepsilon(600\text{ nm}) = -16 - 0.44i$], being the only effect a reduction in the transmitted power. Moreover the decay length of the fundamental mode of the waveguides with $\varepsilon_2 = 1.5$ dielectric core is, for example, $L_D(600\text{ nm}) = [2Im(k_z)]^{-1} = 11.95$ μm, much longer than the device length, indicating that all the relevant dynamics can take place without being suppressed by absorption.

We conclude this section reminding that, as said in Section 2, diffraction curves of the array are not sensitive on nonuniformity consisting in the different width of adjacent cores: in Fig. 12 an example is shown in which cores have different widths $2b = 120$ nm (fixed) and $2c$ that sweeps from 120 nm to 180 nm. On the contrary, dielectric is constant in all cores and is set to 1.0. As we can see, diffraction curves, numerically calculated with a mode solver, change not too much even when $2b$ and $2c$ are very different.

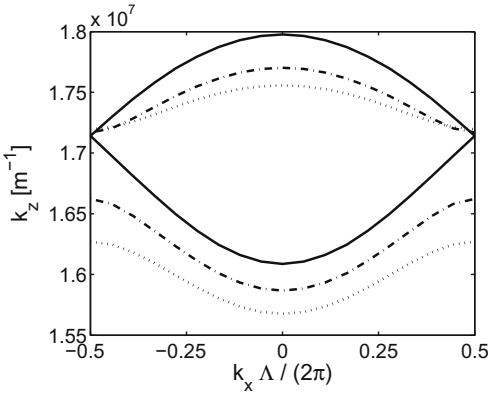

Fig. 12. Diffraction curves of a plasmonic array with different widths of adjacent cores. Widths are alternately $2b = 120$ nm and $2c$ that sweeps from 120 nm to 180 nm. Dielectric constants of the cores: $\varepsilon_1 = \varepsilon_2 = 1.0$. Wavelength $\lambda = 450$ nm. Solid lines for $2c = 120$ nm; dashed line for $2c = 150$ nm; dotted lines for $2c = 180$ nm.

6. Conclusions

In this paper we studied nonuniform plasmonic arrays. We have found that diffraction curves of the array modes are very sensitive to non uniformity consisting in the alternation of two different dielectrics ε_1 and ε_2 in the cores of the array, while not to nonuniformity consisting in the alternation of different widths of cores.

In order to overcome problems arising from the CMT model whose basic cell is the single waveguide, we proposed a CMT model where the basic cell is the unperturbed coupler. We noticed that even for little non uniformity the shape of diffraction curves is sinusoidal and depends only on the couplings between equal modes in adjacent couplers; these couplings can assume different values, entailing different amplitudes for the two diffraction curves. We have seen that the trend of coupling coefficients as function of nonuniformity (that is $\varepsilon_2 - \varepsilon_1$) depends quite exclusively on how modes of unperturbed basic coupler concentrate energy at its interfaces. In the last section, basing on all results obtained, we proposed an example of a flat-diffraction array in the visible band, showing the correctness of all predictions done in the previous sections.

Appendix

In a single plasmonic guide formed by a dielectric layer $2b$ wide, with relative dielectric constant ε and surrounded by metal with relative dielectric constant ε_m, the fundamental mode is TM-even one. Imposing the continuity of the tangential electric and magnetic fields, whose propagation constant is β, we find that:

$$\frac{T_d b}{T_m b} = \frac{\varepsilon}{|\varepsilon_m| \tanh(T_d b)}, \tag{19}$$

where T_d and T_m are the decaying constant of the field in dielectric and metal respectively, with $T_d = \sqrt{\beta^2 - (\omega/c_0)^2 \varepsilon}$ and $T_m = \sqrt{\beta^2 - (\omega/c_0)^2 \varepsilon_m}$. Substituting $T_d b = x$ and $k^2 = (w/c_0)^2(|\varepsilon_m| + \varepsilon)b$ we obtain:

$$\frac{x}{\sqrt{x^2 + k^2}} = \frac{\varepsilon}{|\varepsilon_m| \tanh(x)}. \tag{20}$$

When $\varepsilon/|\varepsilon_m| < 0.5$ we can approximate left and right hand side of Eq. (20) with $(1/k)x$ and $(\varepsilon/|\varepsilon_m|)(1/x)$ respectively, and k with $w_p b/c_0$. In this way we found that $x = \sqrt{\varepsilon k/|\varepsilon_m|}$, then we obtain approximated solutions for the decaying and propagation constants:

$$\begin{aligned} T_d &\approx \sqrt{\frac{\varepsilon w_p}{|\varepsilon_m| b c_0}} \\ T_m &\approx \frac{w_p}{c_0}, \\ \beta &\approx \sqrt{\varepsilon}\sqrt{\left(\frac{\omega}{c_0}\right)^2 + \left(\frac{\omega_p}{|\varepsilon_m| c_0 b}\right)}. \end{aligned} \tag{21}$$

References

[1] S.A. Maier, Plasmonics: Fundamentals and Applications, Springer, 2007.
[2] E.N. Economu, Phys. Rev. 182 (1969) 539.
[3] J.N. Anker, W.P. Hall, O. Lyanders, N.C. Shan, J. Zhao, R.P. Van Duyne, Nature Mater. 7 (2008) 442.
[4] N. Fang et al., Science 308 (2005) 534.
[5] E. Ozbay, Science 311 (2006) 189.
[6] D.N. Christodoulides, R.I. Joseph, Opt. Lett. 13 (1988) 794.
[7] H.S. Eisenberg, Y. Silberberg, R. Morandotti, A.R. Boyd, J.S. Aitchison, Phys. Rev. Lett. 81 (1998) 3383.
[8] W. Lin, X- Zhou, G.P. Wang, C.T. Chan, Appl. Phys. Lett. 91(1–4) (2007) 243113.
[9] A.R. Davoyan, I.V. Shadrivov, A.A. Sukhorukov, Y.S. Kivshar, Appl. Phys. Lett. 94 (2009) 161105.
[10] A.R. Davoyan, A.A. Sukhorukov, I.V. Shadrivov, Y.S. Kivshar, Phys. Rev. A 79 (2009) 013820.
[11] X. Fan, G.P. Wang, J.C. Wai Lee, C.T. Chan, Phys. Rev. Lett. 97 (2006) 073901.
[12] M. Conforti, M. Guasoni, C. De Angelis, Opt. Lett. 33 (2008) 2662.
[13] L. Verslegers, P.B. Catrysse, Z. Yu, S. Fan, Phys. Rev. Lett. 103 (2009) 033902.
[14] G. Bartal, G. Lerosey, X. Zhang, Phys. Rev. B 79 (2009) 201103(R).
[15] A.A. Sukhorukov, Y.S. Kivshar, Opt. Lett. 27 (2002) 2112.
[16] S. Longhi, Opt. Lett. 31 (2006) 1857.
[17] H. Kosaka et al., Appl. Phys. Lett. 74 (1999) 1212.
[18] A. Hardy, W. Streifer, J. Lightwave Technol. LT-3 (5) (1985) 1135.
[19] M. Guasoni, A. Locatelli, C. De Angelis, J. Opt. Soc. Am. B 25 (9) (2008) 1515.
[20] <http://www.comsol.com>.
[21] P.B. Johnson, R.W. Christy, Phys. Rev. B 6 (1972) 4370.